ACS Sustainable Chemistry & Engineering

Research Article

pubs.acs.org/journal/ascecg

A Method for Synthesis of Renewable Cu_2O Junction Composite Electrodes and Their Photoelectrochemical Properties

SocMan Ho-Kimura,*[,†] Savio J. A. Moniz,[‡] Junwang Tang,[‡] and Ivan P. Parkin[†]

[†]Department of Chemistry, University College London, 20 Gordon Street, London WC1H 0AJ, United Kingdom

[‡]Department of Chemical Engineering, University College London, Torrington Place, London WC1E 7JE, United Kingdom

Supporting Information

ABSTRACT: We present a highly active copper oxide composite photoelectrode with improved stability and photoelectrochemical performance brought about by a simple cycle of heat treatment and cathodic reduction. Under one sun (AM 1.5 G, 100 mW/cm^2) light illumination, the photocurrent density of a $Cu_2O/CuO/Al_2O_3$ composite electrode was enhanced to −1.8 mA/cm^2 at 0 V vs RHE compared to −0.25 mA/cm^2 of the native Cu_2O film. The improved stability of the film was demonstrated by ∼60% retention of initial photocurrent (−1.1 mA/cm^2) after 20 sequential cyclic voltammetry scans. Moreover the photocurrent showed only a slight decrease in activity after five regeneration cycles. Furthermore, a high incident photo-to-current efficiency (IPCE, 53% at 450 nm) was recorded. These enhancements in both photocurrent and stability are due to electron transfer from Cu_2O to CuO and increase of carrier density due to the presence of Al_2O_3.

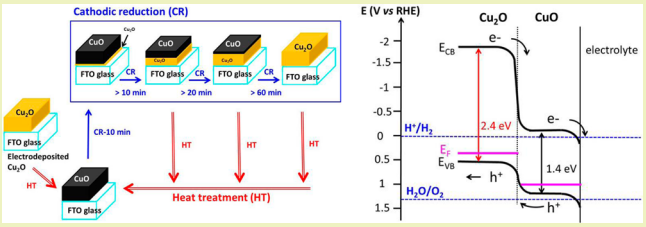

KEYWORDS: *Photocatalysis, Heterojunction, Solar energy, Thin films, Electrochemistry*

INTRODUCTION

Hydrogen production and carbon dioxide reduction over semiconductor photocatalysts is believed to be a promising method to generate clean, sustainable energy supplies as an alternative to the combustion of finite resources, such as fossil fuels.[1] Photocatalytic and photoelectrochemical (PEC) water oxidation on *n*-type oxide semiconductors has been extensively investigated since the discovery of PEC water splitting on TiO_2 with a Pt counter electrode by Honda and Fujishima[2] in the early 1970s. Materials such as TiO_2,[3] ZnO,[4] Fe_2O_3,[5] WO_3,[6] and $BiVO_4$[7] have been reported for PEC water oxidation, while comparatively fewer *p*-type materials have been reported; there appears to be a handful of reports published on the synthesis of photocathode materials based on Cu compounds.[8,9] Copper(I) oxide (Cu_2O) is a well-known, earth-abundant *p*-type semiconductor with a band gap of about 2 eV, making it a good fit for solar-driven water splitting under visible light. In addition, Cu_2O has a suitably negative conduction band position with sufficient overpotential for H_2 production and has been reported to possess a maximum theoretical photocurrent of −14.7 mA/cm^2 and light-to-hydrogen conversion efficiency of 18.7%.[10] However, a major drawback of Cu_2O is its facile photocorrosion in solution. For example, a bare Cu_2O photocathode only displayed a photoresponse for about 5 min irradiation due to reduction to Cu metal.[10] Other studies have reported that growing a thin protective layer on Cu_2O results in improved photoactivity and stability; single layers of TiO_2[11] and WO_3[12] and multilayers of TiO_2, ZnO, and Al_2O_3,[10] and CuO nanowires[13,14] on Cu_2O have all been demonstrated in this regard. In general, loading a material with a more positive conduction band onto Cu_2O creates a junction at the interface of the two materials that can reduce photodegradation through transferring electrons away from Cu_2O. Likewise, a previous report showed that Cu_2O heated under nitrogen atmosphere exhibited an increased incident photon-to-electron conversion efficiency (IPCE) from 2% to 9% at 550 nm.[15]

Copper(II) oxide (CuO) is an intrinsic *p*-type semiconductor with a band gap of 1.3−1.7 eV,[16] enabling good solar light harvesting. However, the conduction band position of CuO is not sufficiently negative enough to reduce protons to H_2 gas.[17] In this regard, CuO has recently been incorporated into many heterojunction composite photocatalysts, such as Cu_2O/CuO[13,14] and CuO/ZnO.[19] In fact CuO/TiO_2[17] and CuO-loaded $La_2Ti_2O_7$[18] both show improved activity for hydrogen evolution under UV light irradiation.

It has been reported that some other metal oxide (MO) layers can suppress photocorrosion and can be a protection layer for Cu_2O.[10−12] In this regard, atomic layer deposition (ALD) has been used to coat multiple metal oxide layers on the surface of Cu_2O films;[10] however, ALD deposition rates are at present too low for large area deposition. In the present study, we develop a simple, cheap methodology to prepare $Cu_2O/CuO/MO$ composite photocathodes that are significantly more resistant to corrosion than bare Cu_2O. Furthermore, if corroded, these electrodes can be simply regenerated through a cycle of heat treatment and cathodic reduction. MO (M = Ti,

Received: January 9, 2015
Revised: February 20, 2015
Published: February 25, 2015

DOI: 10.1021/acssuschemeng.5b00014
ACS Sustainable Chem. Eng. 2015, 3, 710−717

Zn, Al) species were also formed on the Cu_2O/CuO composite, with Cu_2O/CuO/Al_2O_3 in particular demonstrating superior photoelectrochemical properties.

EXPERIMENTAL SECTION

Film Growth. Three micrometer thick Cu_2O films (area of about 1.0 cm × 1.5 cm) were fabricated by galvanostatic deposition at 65 °C. The bath was an aqueous solution containing 0.2 M copper(II) sulfate pentahydrate (Sigma-Aldrich) and 1.5 M lactic acid (Sigma-Aldrich) from a pH range of 10 to 12.5 (adjusted with 5 M NaOH). A conductive fluorine-doped tin oxide glass (FTO glass, TEC15, NSG) was used as the substrate. Prior to the deposition, the FTO glass substrates were sonicated in acetone and distilled water for 30 min each, dried in air, and then placed in a furnace at 400 °C for 30 min. The cathodic deposition was carried out by galvanostatic mode. A 5 cm^2 Pt gauze was used as the counter electrode. The Cu_2O films were deposited at constant current density of −0.3 mA/cm^2, approximately the electric charge was 2 C/cm^2.

Titanium dioxide (TiO_2), zinc oxide (ZnO), and aluminum oxide (Al_2O_3) were used as metal oxide (MO) species. MO species were coated by drop-casting the precursor onto electrodeposited Cu_2O film and then dried at room temperature. All the Cu_2O with MO species electrodes were annealed at 550 °C for 60 min (5 °C/min) in air. The 0.25 wt % TiO_2 source, peroxotitanic acid, was prepared by dissolving amorphous titanium dioxide into hydrogen peroxide (Sigma-Aldrich, 30 wt % in H_2O) in an ice bath.[21] A 0.24 M zinc acetate dihydrate in methanol was used for ZnO growth.[22] The aluminum oxide precursor solution was prepared using 0.01 M aluminum nitrate nonahydrate (Sigma-Aldrich) in methanol (Sigma-Aldrich).

The thickness of the Cu_2O layer and CuO layer of the Cu_2O/CuO/MO composite film was controlled by cathodic reduction. The cathodic reduction was carried out in a 1 M sodium hydroxide solution at constant current densities of about −0.3 mA/cm^2 for 20 and 60 min (electric charge was between 0.36 and 1.08 C/cm^2) at 65 °C without stirring. A 5 cm^2 Pt gauze was used as the counter electrode.

Photoelectrochemical Measurements. The photoresponse of the Cu_2O/CuO films was measured using a 100 W Xe lamp fitted with a monochromator (Newport, 66450 Apex Arc Lamp Sources) an AM 1.5G filter and a home-built programmable light chopper (Orientalmotor). The light output was calibrated to 1 sun (100 mW/cm^2). The photoelectrochemical performance of the films was evaluated in a three-electrode configuration using a potentiostat/galvanostat/impendance analyzer (palmSens+3). The reference electrode was Ag/AgCl in 3 M KCl (BaSi, Inc., U.K.), and a 5 cm^2 Pt gauze was used as the counter electrode. Films were illuminated from the FTO glass substrate side (SE illumination). The scan rate for cyclic voltammetry was 10 mV/s. The electrolyte was comprised of a 0.5 M Na_2SO_4 solution (pH 6). IPCE measurements were carried out every 25 nm from 400 to 700 nm by measuring the photocurrent produced under chopped monochromatic light irradiation (Newport, 74125 Oriel Cornerstone 260 1/4 m Monochromator; with a 395 nm long pass filter, UQG Optics, GG395 Yellow Schott Optical Filters) at a fixed electrode potential of 0 V vs RHE. All the potentials in this work are reported against the reversible hydrogen electrode, obtained from those relative to the Ag/AgCl reference electrode using the Nernst equation, $E_{RHE} = E^0_{Ag/AgCl} + E_{Ag/AgCl} + 0.059$ pH, where E_{RHE} is the converted potential vs RHE, $E^0_{Ag/AgCl} = 0.1976$ at 25 °C, and $E_{Ag/AgCl}$ is the experimentally measured potential against Ag/AgCl reference. Monochromatic light intensity was measured with a hand-held optical photometer (Thorlabs, PM100A) and a calibrated photodiode power sensor (Thorlabs, S120VC). The dark/light cycles were set at 10/10 s. IPCE (%) was calculated from eq 1:

$$\mathrm{IPCE}\,(\lambda) = \frac{1240 j(\lambda)}{I_0(\lambda) \times \lambda} \times 100\% \tag{1}$$

where λ is the wavelength of incident monochromatic light (nm), $j(\lambda)$ is the photocurrent density under illumination at wavelength λ (mA/cm^2), and $I_0(\lambda)$ is the incident light intensity at wavelength λ (mW/cm^2). Mott−Schottky plots (capacitance−potential curves) were recorded of the impedance in the dark at a frequency of 1 k Hz with AC amplitude of 5 mV. Equation 2 was used to determine flat band potential (V_{fb}) and carrier density (N_A).

$$\frac{1}{C^2} = \frac{2}{\varepsilon_0 \varepsilon_r e N_A}\left(V - V_{fb} - \frac{k_B T}{e}\right) \tag{2}$$

Here N_A is the carrier density, ε_0 is the permittivity in vacuum; ε_r is the relative permittivity; V is the applied potential, T is the absolute temperature, e is the electronic charge, and k_B is the Boltzmann constant.

Film Characterization. Electron micrographs of the samples were obtained on a JEOL, JSM-6700F field emission scanning electron microscope (SEM), operated in gentle beam mode (8 mm stage height, 0° stage tilt, and 5 kV acceleration voltage 10 mA current) to minimize surface charging effect. Phase identification of the films was achieved using a Bruker D8 discovery X-ray diffractometer (XRD) equipped with Cu Kα (λ = 1.541 Å) radiation, operated on 2 θ scan mode from 15 to 66° 2 θ, tube at 1°, 0.05° step size, and 2 s per step. To confirm Cu_2O and CuO, reference JCPDS file No. 65-3288 and JCPDS file No. 05-0661, respectively, are cited. UV−vis absorption spectra of the films were analyzed using a Lambda 950 (PerkinElmer) UV−vis spectrophotometer with an integrating sphere, operated in transmission mode. X-ray photoelectron spectroscopy (XPS) data were collected by a Thermo Scientific K-Alpha X-ray photoelectron spectrometer under ultrahigh vacuum (<5 × 10^8 Torr) and by using a monochromatic Al Kα X-ray source. The adventitious carbon 1s peak was calibrated to 285 eV and used as an internal standard to compensate for any charging effects.

RESULTS AND DISCUSSION

Effect of Cathodic Reduction. All electrodeposited Cu_2O films were made by a modified literature method.[23,24] As displayed in Figure S1 of the Supporting Information, XRD patterns and SEM images indicated a [111] preferred orientation was dominant when the bath pH is higher than 12.5. In the cases where the pH is equal to or lower than 10, the [200] facet becomes dominant. The main crystallographic plane is greatly determined by the concentration of hydroxyl ions, growth rate of the film, and number of oxygen atoms per unit area.[24] CuO has been reported to act as a protective layer on Cu_2O to stop corrosion;[13,14,25] therefore, in order to configure the Cu_2O/CuO layers, we developed a novel method comprising heat treatment (HT) followed by cathodic reduction (CR). To transform Cu_2O to CuO ($2Cu_2O + O_2 \rightarrow 4CuO$), electrodeposited Cu_2O films were placed in a furnace at 450 °C for 30 min in air. To control the ratio of CuO to Cu_2O/CuO, films were reduced to Cu_2O by cathodic reduction. The cathodic reduction took place through the reaction of Cu(II) → Cu(I), E = 0.36 V vs RHE and Cu(I) → Cu(0), E = −3.2 V vs RHE.[13] The protocol was carried out in a 1 M sodium hydroxide solution (pH 13.6, 65 °C) at constant current densities (−0.26 mA/cm^2) by means of galvanostatic reduction. The ratio of Cu_2O to CuO was controlled by the duration of reduction (Figure 1a). The Cu_2O component increased with reduction time, and after 50 min, XRD revealed very weak intensity peaks assigned to CuO. While we could not determine the Cu_2O to CuO ratio using this method, the peak intensities revealed some Cu_2O transformation to CuO by heat treatment, followed by CuO reduction back to Cu_2O by cathodic reduction. Figure 1b shows the XRD patterns of Cu_2O [111] from the cycle of heat treatment and cathodic reduction using the same sample in a continuous manner. This is a reversible transformation and therefore facilitates renewal of a Cu_2O/CuO junction photocathode. XRD data of Cu_2O [200] films after HT and varying CR times are shown in Figure S2 of

DOI: 10.1021/acssuschemeng.5b00014
ACS Sustainable Chem. Eng. 2015, 3, 710−717

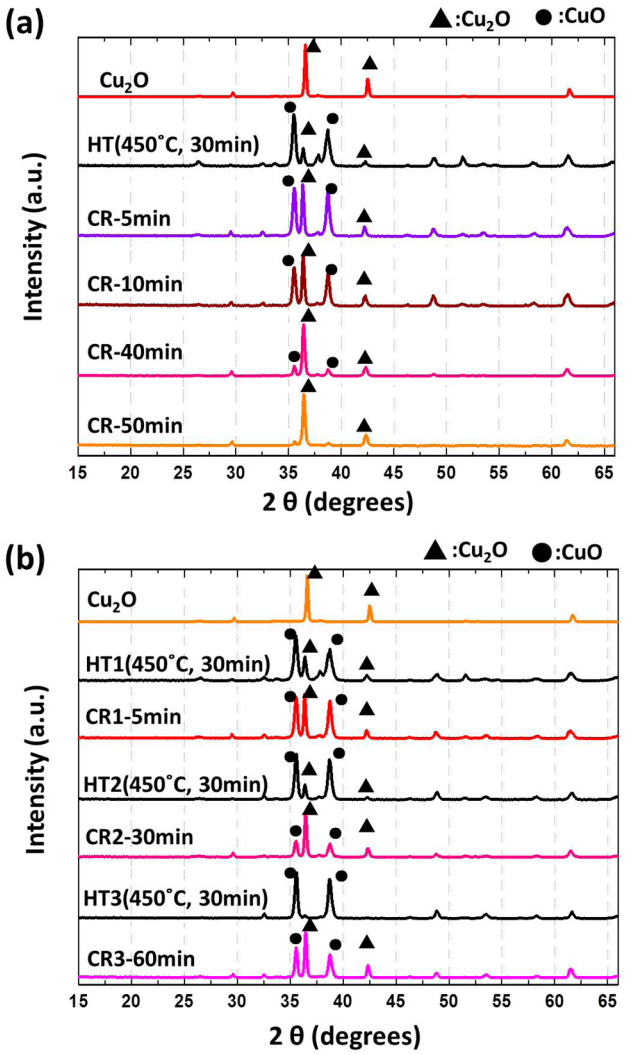

Figure 1. (a) XRD pattern of Cu_2O [111] after heat treatment (HT) at different cathodic reduction (CR) times. (b) XRD patterns from the repeat cycle of heat treatment and cathodic reduction.

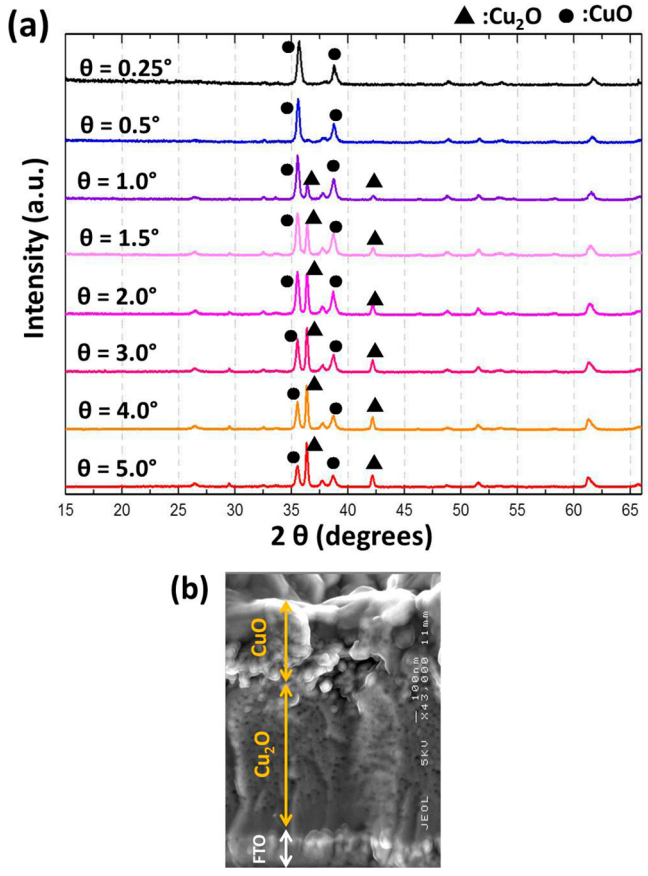

Figure 2. (a) Depth profile XRD patterns. Shallow incidence X-ray (θ = 0.25°) pattern shows CuO on the surface of the sample. Deep incidence (θ = 5°) pattern shows Cu_2O/CuO composite in the bulk part of the sample. This sample was obtained after a CR-60 min treatment. (b) SEM cross-section image of the sample.

the Supporting Information. In the same manner as cathodic reduction in 1 M sodium hydroxide solution, when CuO is reduced to Cu_2O, not only was the [200] plane observed but the [111] was also prominent. The trend is rationalized in terms of the bath pH value. It is probable that the growth rates of [200] and [111] are determined by the concentration of hydroxyl ions and are the same phenomenon as electrodepositing a Cu_2O film as demonstrated above. In this work, we did not see a noticeable change in the photoresponse with material crystallinity of the electrodeposited Cu_2O. Furthermore, if the cathodic reduction occurs in an acidic solution under the same conditions, CuO will be rapidly reduced to copper metal, which will lead to its delamination from the substrate (Figure S3, Supporting Information).

Figure 2a shows XRD depth profiles collected from different angles (θ) of incidence X-ray to the sample surface. A Cu_2O/CuO film formed after heat treatment at 550 °C for 1 h then cathodic reduction for 60 min was investigated. At lower measurement angles, XRD data is obtained predominantly from species closer to the surface. In contrast, when the angle is larger, XRD data are obtained not only from the surface but also from the bulk of the sample. Here, the shallow incidence X-ray (θ = 0.25°) pattern clearly shows crystallized CuO on the surface of the sample, and a larger angle of incidence (θ = 5°) results in the Cu_2O/CuO composite in the bulk of the sample. During the cathodic reduction, the CuO was initially reduced from the side nearest the conductive FTO layer. As a consequence, a two-layer Cu_2O/CuO junction electrode was obtained, with Cu_2O on the bottom and CuO on the top surface. Additionally, from the bottom to the top surface of the sample, the XRD intensity of Cu_2O decreased gradually to zero as CuO was cathodically reduced to Cu_2O from the bottom. EDX analysis revealed, as expected, the presence of copper and oxygen in a 1:1 ratio at the top and a 2:1 atomic ratio on the bottom of the Cu_2O/CuO composite, indicating Cu_2O nearest the FTO glass (Figures S4 and S5 and Table S1, Supporting Information). Furthermore, the SEM cross-section image provides further evidence for the formation of two layers (Figure 2b). The thickness of Cu_2O is about 2 μm, and thickness of CuO is about 1 μm.

PEC Performance. To avoid the top CuO layer blocking incident photos, all PEC measurements are carried out with irradiation from the FTO glass substrate side. In Figure 3a, the photocurrent density of Cu_2O and Cu_2O/CuO CR-0 min (after heating at 550 °C for 1 h without cathodic reduction) and Cu_2O/CuO CR-60 min (after heating at 550 °C for 1 h then cathodic reduction for 60 min) films were measured. Electrodeposited Cu_2O and Cu_2O/CuO (CR-0 min) exhibited very poor performance. Especially, the Cu_2O/CuO (CR-0 min)

DOI: 10.1021/acssuschemeng.5b00014
ACS Sustainable Chem. Eng. 2015, 3, 710−717

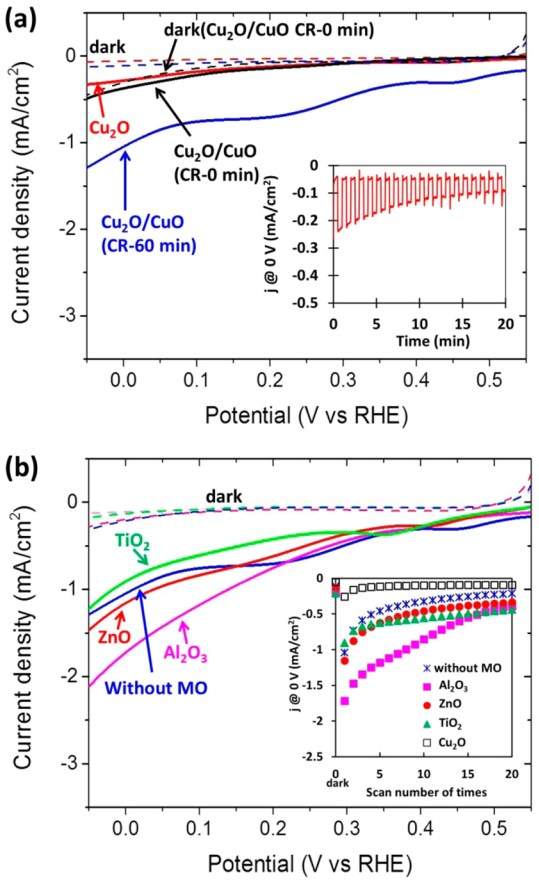

Figure 3. (a) Photoelectrochemical response of Cu_2O and Cu_2O/CuO composite of cathodic reduction 0 and 60 min. (b) First $J-V$ curve of 20 CVs of Cu_2O/CuO/MO (CR-60 min) films, MO = Al_2O_3, ZnO, and TiO_2. Dashed line: dark measurements. Solid line: light measurements. Inset: Stability of photocurrent density at a potential of 0 V with (a) Cu_2O film stability for 20 min under chopped light and (b) 20 CV scans.

sample displayed a high dark current. The Cu_2O/CuO CR-60 min film showed negligible dark current and high photocurrent density, revealing that this bilayer junction composite works effectively. This is most probably due to facile electron transfer from Cu_2O to CuO through to the electrolyte. The $J-T$ stability of a Cu_2O film showed very low photoresponse at the end of 20 min illumination (Figure 3-a, inset). In addition, this Cu_2O film was not able to produce a photocurrent again after the initial measurement. The Cu_2O/CuO composite formed from cathodic reduction for 60 min without the MO electrode showed significantly improved performance compared to the native Cu_2O, increasing from −0.25 to −1.4 mA/cm^2 at 0 V vs RHE. These results suggest that the CuO layer functions as an electron acceptor and passivation layer that substantially decreased the photocorrosion of Cu_2O.[13,14,25]

Paracchino et al. investigated a multilayer photoelectrode of Cu_2O/5 × (4 nm ZnO/0.17 nm Al_2O_3)/11 nm TiO_2/ Pt.[10] The multilayer electrode represented a 3-fold higher photocurrent at 0 V vs RHE compared to the electrodeposited Cu_2O film. However, there are no reports on alumina (Al_2O_3) individually acting as a protective species in this context. In this work, we probed the effect of Al_2O_3, ZnO, and TiO_2 on the PEC performance of copper oxide composites. Precursors to TiO_2, ZnO, and Al_2O_3 were coated on electrodeposited Cu_2O film through drop-casting. Cu_2O/CuO/MO (M = Ti, Zn, Al) films were formed after heat treatment at 550 °C for 1 h followed by 60 min of cathodic reduction in 1 M NaOH solution at 65 °C. PEC measurements were performed on these Cu_2O/CuO/MO (CR-60 min) films. The first $J-V$ scan of 20 CV curves is shown in Figure 3b; changes of photocurrent density at 0 V of 20 CVs were observed for the stability test (Figure 3b, inset). The $J-V$ curves of the Cu_2O/CuO/Al_2O_3 exhibited a photocurrent of −1.8 mA/cm^2 at 0 V vs RHE, representing a more than 7-fold improvement compared to the bare Cu_2O. Photoactivity of these samples decayed after 20 CVs through photocorrsion to Cu metal, which was confirmed by XRD (not shown herein). The photoactivity of Cu_2O/CuO and Cu_2O/CuO/MO composites decayed much more slowly than the native Cu_2O film, and this is due to the protection effect from the CuO layer and the high conductivity of the metal oxide. Somewhat surprisingly, ZnO and TiO_2 do not significantly increase the photocurrent density of Cu_2O/CuO junction electrode. In fact, TiO_2 appears to suppress photoactivity, most probably through acting as a recombination center; however, both ZnO and TiO_2 can partially improve stability compared to the bare Cu_2O (Figure 3b, inset). In contrast, Al_2O_3 greatly increases the photocurrent and improves the stability. In comparison, the bare Cu_2O film exhibited almost no photoresponse after 5 CV scans. Al_2O_3-doped ZnO with an increased carrier density and carrier mobility has been reported by others.[26,27] Al_2O_3 on TiO_2 has also been reported to act as a barrier to charge recombination, with a notably improved electron lifetime compared to bare TiO_2.[28] Additionally, adding an Al_2O_3 layer has been shown to increase conductivity and minimize surface charge recombination on *p*-NiO[29] and to significantly increase the photocurrent of *p*-SiO.[30] Hence, we believe that the action of Al_2O_3 is most likely to increase photoconductivity at the surface of the Cu_2O/CuO electrode for efficient transfer at the surface of CuO, rather than acting as a protection layer.

We probed the exact nature of the chemical species in the Cu_2O/CuO/Al_2O_3 (CR-0 min) composite (HT: 550 °C, 1 h without cathodic reduction) via XPS (Figure 4). The Cu 2p core level revealed the presence of CuO from the Cu $2p_{1/2}$ and Cu $2p_{3/2}$ peaks at 954.4 and 934.6 eV, indicating the presence of Cu^{2+}. Additionally, two strong satellite peaks were observed at 962.4 and 942.3 eV. However, from the peak fitting and peak broadening for Cu $2p_{1/2}$ and Cu $2p_{3/2}$, we found two other additional peaks at binding energies of 952.5 and 932.7 eV, attributed to Cu_2O. This shows that electrodeposited Cu_2O was not completely oxidized to CuO after heat treatment at 550 °C for 1 h in air. The Al $2p_{1/2}$ peak was found at 74.4 eV, commensurate with Al_2O_3, but with an additional yet unassigned peak at 77.4 eV. Unsurprisingly, no crystalline Al_2O_3 was detected from XRD due to the low temperature of heat treatment (Figure S6, Supporting Information). On the other hand, Al was detected from this Cu_2O/CuO/Al_2O_3 sample by EDX measurement, resulting in a ratio of Cu:Al:O = 45:4:51 atom % (Figure S7, Supporting Information). There is only a small amount of Al_2O_3 was loaded on the surface of CuO. However, all the Cu_2O/CuO composites were deposited on FTO glass substrates, and furthermore, surface oxygen contamination is always present. Thus, oxygen quantification from XPS and EDX measurements would be unreliable in this case.

Photocurrent density potential ($J-V$) curves of Cu_2O/CuO/Al_2O_3 films were collected from a series of different cathodic reduction durations (Figure S8, Supporting Information). A

DOI: 10.1021/acssuschemeng.5b00014
ACS Sustainable Chem. Eng. 2015, 3, 710−717

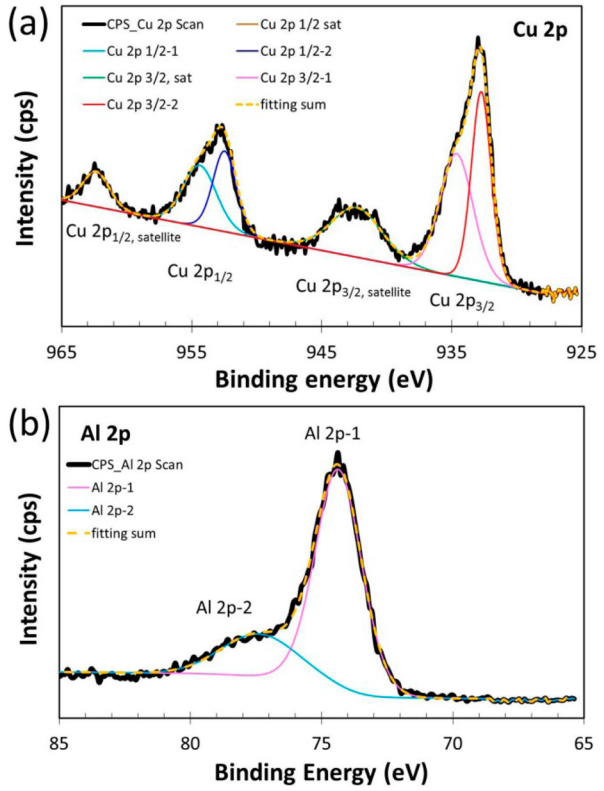

Figure 4. XPS spectra of (a) Cu 2p and (b) Al 2p obtained from the $Cu_2O/CuO/Al_2O_3$ (HT: 550 °C, 1 h without cathodic reduction) film.

high dark current was obtained from a $Cu_2O/CuO/Al_2O_3$ (CR-0 min) film without cathodic reduction. This result is similar to Cu_2O/CuO CR-0 min (HT: 550 °C, 1 h without CR, Figure 3a). By comparison with these two films, the effect of loading Al_2O_3 not only increased conductivity in the dark but also increased photocurrent density. When reduction times were longer than 10 min, the dark current was reduced and photocurrent density markedly increased. The optimum period for cathodic reduction appears to be about 60 min. After a 90 min reduction, the photocurrent decreased slightly. It is thought that the reduction reaction "CuO + e → Cu_2O" takes about 60 min for our samples. After 90 min, the reduction of "Cu_2O + e → Cu metal" occurs. For this reason, the decrease of photocurrent is ascribed to the presence of Cu metal. The stability test showed photocurrent decay after 20 CV scans (Figure S8, inset, Supporting Information). In the case of cathodic reduction for 10 and 20 min, there is no significant decrease after 10 scans, and photocurrent densities are still maintained at −1.0 mA/cm^2 at 0 V vs RHE after 20 scans. Thicker CuO layers appear to maintain photocurrents for longer time periods. The thickness of the top protective CuO layer was controlled by a cathodic reduction technique.

For the regeneration test of $Cu_2O/CuO/Al_2O_3$ films, we used the same composite to repeat 20 CV scans followed by heat treatment and cathodic reduction. In Figure 5, five regeneration cycles have been carried out. Figure 5a and b showed the results of cathodic reduction times for 20 and 60 min, respectively. The *J*−*V* curve Round-1 is the first scan of 20 CVs of the initial cycle. After the 20 CV measurements, the photocurrent at 0 V vs RHE decreased substantially (Figure 5, inset). However, the $Cu_2O/CuO/Al_2O_3$ film was heated at 550

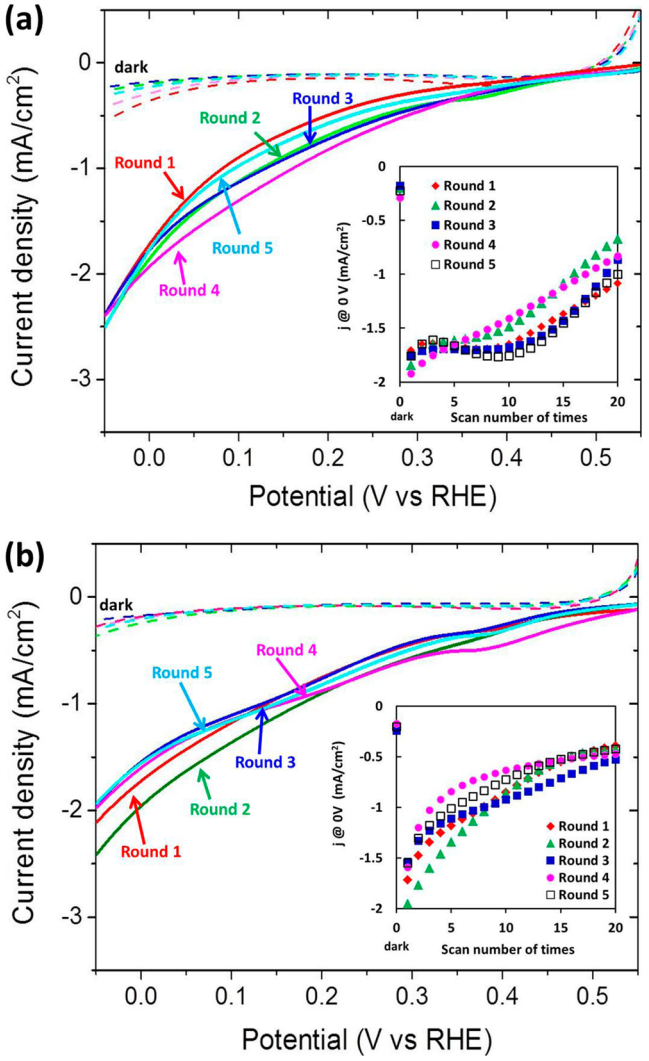

Figure 5. First *J*−*V* curve of $Cu_2O/CuO/Al_2O_3$ films of 20 CVs followed by HT and CR for five repetitions. Inset: Stability variation of photocurrent density at a potential of 0 V. (a) Cathodic reduction time = 20 min. (b) Cathodic reduction time = 60 min.

°C for 1 h and then had cathodic reduction treatment again. The *J*−*V* curve Round-2, the first scan of 20 CVs of the second cycle, showed almost the same level of photoactivity as initial cycle. In the same way, refreshed $Cu_2O/CuO/Al_2O_3$ film of Round-3, Round-4, and Round-5 have been tested (Figure 5a and b). Overall the photocurrent was high without any noticeable decrease in activity after five regeneration cycles. The renewed films display high activity due to oxidation of Cu to CuO by heat in air, followed by cathodic reduction to form Cu_2O/CuO junction.

The *J*−*T* stability and *J*−*V* curves under chopped light illumination were obtained using the same electrodes of Figure 5 (Figure 6). The *J*−*T* stability of $Cu_2O/CuO/Al_2O_3$ (CR-20 min) composite showed about 60% photocurrent density remaining after 20 min of testing. Furthermore, under chopped light illumination, the *J*−*V* curves of the revitalized composites maintained a high level of activity. Cathodic reduction for 60 min resulted in similar photocurrent but lower stability (Figure 6b). The results in Figure 6 agree with the results obtained in Figure 5.

DOI: 10.1021/acssuschemeng.5b00014
ACS Sustainable Chem. Eng. 2015, 3, 710−717

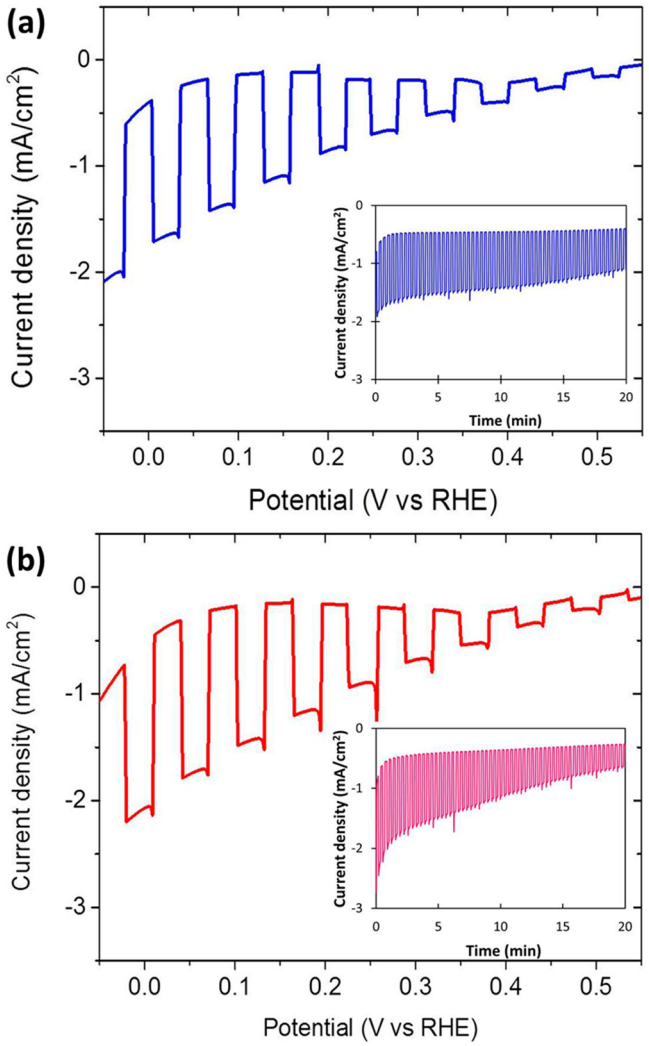

Figure 6. Photoelectrochemical response under chopped light exposure for $Cu_2O/CuO/Al_2O_3$ composite of (a) CR-20 min and (b) CR-60 min films. Inset: Stability evaluation of photocurrent density at a potential of 0 V vs RHE.

UV−vis absorption spectra were recorded for Cu_2O and Cu_2O/CuO (CR-0, 20, 60 min) electrodes (Figure S9, Supporting Information). The band gaps for Cu_2O and Cu_2O/CuO (CR-0, 20, 60 min) were found to be about 2.4 and 1.4 eV, respectively, in agreement with the literature values of Cu_2O and CuO.[10,14,16] Cu_2O films synthesized in this study were orange in color, while Cu_2O/CuO CR-0 min films were almost black in appearance. Junction Cu_2O/CuO films are comprised of two layers, a black CuO on the top and a dark orange Cu_2O on the bottom. Therefore, in order to investigate the light conversion efficiency of these copper oxide based electrodes, the incident photo-to-current efficiency (IPCE) was measured at a potential of 0 V vs RHE. In Figure S10 of the Supporting Information, the IPCE of the unmodified Cu_2O film is very low, about 4% at 400 nm, with no current recorded at $\lambda > 550$ nm, in agreement with its UV−vis absorption spectra (Figure S9, Supporting Information). The maximum IPCE of the $Cu_2O/CuO/Al_2O_3$, CR-60 min and CR-20 min composites were 53% at 450 nm and 40% at 550 nm, respectively (Figure 7). The CR-20 min film exhibited higher IPCE at longer wavelengths, did not fall to zero due to the light absorption of the top CuO layer, and is in agreement with its UV−vis spectra

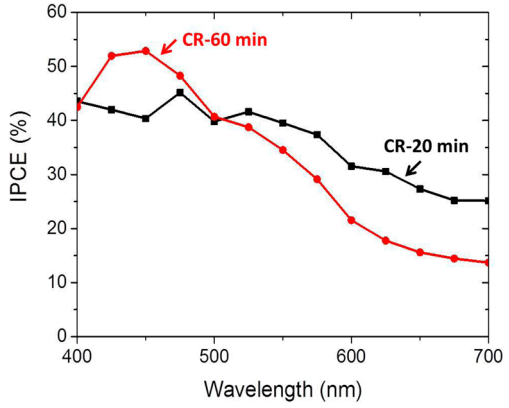

Figure 7. IPCE of Cu_2O-CuO/Al_2O_3 films. Photocurrent densities were measured at a potential of 0 V vs RHE.

(Figure S9, Supporting Information). It is assumed that the excellent efficiency of $Cu_2O/CuO/Al_2O_3$ composites originates from charge transfer in the Cu_2O/CuO junction.

In order to assess the conductivity effects of Al_2O_3 and determine the flat band potentials of copper oxide phases, impedance measurements (Mott−Schottky) were carried out at a frequency of 1 KHz in the dark. The interfacial capacitance (C) was calculated by measured reactance (imaginary part of impedance). The Mott−Schottky Plot is presented in Figure 8.

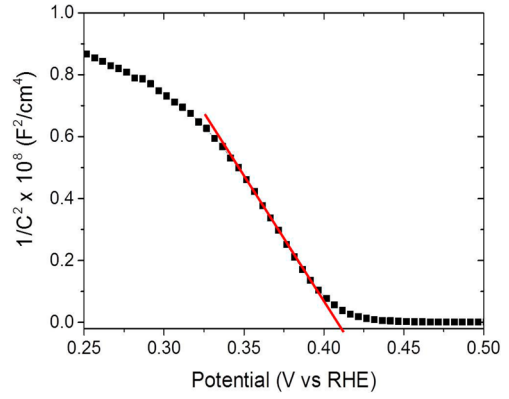

Figure 8. Mott−Schottky Plot of $Cu_2O/CuO/Al_2O_3$ (CR-60 min) electrode.

The flat band potential (V_{fb}) was determined from the intercept of the linear part of the curves (Table S2, Supporting Information). The flat band potentials were estimated to be 0.41 and 1.07 V vs RHE for Cu_2O and Cu_2O/CuO CR-0 min, respectively. The implicit V_{fb} of CR-20 min and CR-60 min $Cu_2O/CuO/Al_2O_3$ films were 0.44 and 0.41 V vs RHE, respectively, and at an equivalent level to unmodified Cu_2O, thus revealing that addition of Al_2O_3 does not shift the V_{fb} of Cu_2O significantly and is similar to that reported for Cu_2O/nanowire CuO films.[13,14] From the flat band potential of p-type semiconductors, one can estimate the valence band position. The valence band for Cu_2O and Cu_2O/CuO (CR-0 min) was calculated to 0.5 and 1.2 eV vs RHE, respectively. The carrier density (N_A) of the electrodes was calculated by the slope of the linear part of the Mott−Schottky Plot from eq 2. The N_A values of the Cu_2O and Cu_2O/CuO (CR-0 min) films are assumed on the order of 10^{16} and 10^{19} cm^{-3}, respectively (ε_r values of Cu_2O and CuO were taken as 7.6 and 18.1) This is in

DOI: 10.1021/acssuschemeng.5b00014
ACS Sustainable Chem. Eng. 2015, 3, 710−717

agreement with previous results of N_A for Cu_2O and CuO, which were 10^{17} and 10^{18} cm^{-3} respectively.[11] Also in agreement with refs13 and14, these reports showed the N_A values of the Cu_2O/nanowire−CuO films were on the order of 10^{19} cm^{-3}. High carrier densities suggest the aluminum species is able to improve conductivity and interfacial charge transfer. Moreover, the range of N_A values of the $Cu_2O/CuO/Al_2O_3$ CR-20 and CR-60 min films were found to be on the order of 10^{23} cm^{-3}, much higher than the $Cu_2O/CuO/Al_2O_3$ CR-0 min films (10^{21} cm^{-3}). Hence, a suggestion of the mechanism for the improvement in PEC activity for our $Cu_2O/CuO/Al_2O_3$ junctions is based upon two factors (Figure S11, Supporting Information). First, light absorption in Cu_2O generates charge carriers whereby electrons can migrate to CuO on the Cu_2O surface, mitigating the photocorrosion of Cu_2O to Cu metal. Second, electrons on the surface of CuO can then be transferred to the electrolyte for efficient proton reduction to H_2 or other reactions. Photoconductivity in the junction Cu_2O/CuO is enhanced by the introduction of Al_2O_3 species, which improves conductivity and could further act as an electron acceptor.

CONCLUSIONS

In the present work, a simple novel approach of producing copper oxide composite photocathodes is presented, and their recycling is demonstrated through a cycle of oxidation and cathodic reduction. Formation of a thick CuO layer on Cu_2O by this process resulted in improved photocurrent and stability due to the formation of a heterojunction at the surface. In addition, a small quantity of aluminum species also improved the PEC performance. We attribute this enhancement to the formation of a triple junction $Cu_2O/CuO/Al_2O_3$ electrode that allows for facile electron transfer from Cu_2O to CuO and improved photoconductivity brought about by the incorporation of alumina species. Therefore, we demonstrate a simple yet effective strategy to improve the stability and photocurrent generation in Cu_2O photocathodes for renewable energy applications.

ASSOCIATED CONTENT

Supporting Information

Material as mentioned in the text. This material is available free of charge via the Internet at http://pubs.acs.org.

AUTHOR INFORMATION

Corresponding Author

*E-mail: s.kimura@ucl.ac.uk.

Notes

The authors declare no competing financial interest.

ACKNOWLEDGMENTS

EPSRC is thanked for funding (EPSRC grant code EP/J500136/1), and we thank Nuruzzaman Noor for XPS measurement support. S.M. is grateful to EU FP7 for funding (4G PHOTOCAT 309636).

REFERENCES

(1) Moniz, S.; Shevlin, S.; Martin, D.; Guo, Z.-X.; Tang, J. Visible-light driven heterojunction photocatalysts for water splitting − A critical review. *Energy Environ. Sci.* **2015**, DOI: 10.1039/C4EE03271C.

(2) Fujishima, A.; Honda, K. Electrochemical photolysis of water at a semiconductor electrode. *Nature* **1972**, *238*, 37−38.

(3) Carmichael, P.; Hazafy, D.; Bhachu, D.; Mills, A.; Darr, J.; Parkin, I. Atmospheric pressure chemical vapour deposition of boron doped titanium dioxide for photocatalytic water reduction and oxidation. *Phys. Chem. Chem. Phys.* **2013**, *15*, 16788−16794.

(4) Wolcott, A.; Smith, W.; Kuykendall, T.; Zhao, Y.; Zhang, J. Photoelectrochemical study of nanostructured ZnO thin films for hydrogen generation from water splitting. *Adv. Funct. Mater.* **2009**, *19*, 1849−1856.

(5) Pendlebury, S.; Cowan, A.; Barroso, M.; Sivula, K.; Ye, J.; Grätzel, M.; Klug, D.; Tang, J.; Durrant, J. Correlating long-lived photogenerated hole populations with photocurrent densities in hematite water oxidation photoanodes. *Energy Environ. Sci.* **2012**, *5*, 6304.

(6) Cole, B.; Marsen, B.; Miller, E.; Yan, Y.; To, B.; Jones, K.; Al-jassim, M. Evaluation of nitrogen doping of tungsten oxide for photoelectrochemical water splitting. *J. Phys. Chem. C* **2008**, *112*, 5213−5220.

(7) Ho-Kimura, S.; Moniz, S.; Handoko, A.; Tang, J. Enhanced photoelectrochemical water splitting by nanostructured $BiVO_4$−TiO_2 composite electrodes. *J. Mater. Chem.* **2014**, *2*, 3948−3953.

(8) Halmann, M. Photoelectrochemical reduction of aqueous carbon dioxide on p-type gallium phosphide in liquid junction solar cells. *Nature* **1978**, *275*, 115−116.

(9) Mor, G.; Varghese, O.; Wilke, R.; Sharma, S.; Shankar, K.; Latempa, T.; Choi, K.; Grimes, C. p-Type Cu-Ti-O nanotube arrays and their use in self-biased heterojunction photoelectrochemical diodes for hydrogen generation. *Nano Lett.* **2008**, *8*, 1906−1911.

(10) Paracchino, A.; Laporte, V.; Sivula, K.; Grätzel, M.; Thimsen, E. Highly active oxide photocathode for photoelectrochemical water reduction. *Nat. Mater.* **2011**, *10*, 456−461.

(11) Huang, Q.; Kang, F.; Liu, H.; Li, Q.; Xiao, X. Highly aligned Cu_2O-CuO/TiO_2 core/shell nanowire arrays as photocathodes for water photoelectrolysis. *J. Mater. Chem. A* **2013**, *1*, 2418−2425.

(12) Martinez-Garcia, A.; Vendra, V.; Sunkara, S.; Haldankar, P.; Jasinski, J.; Sunkara, M. Tungsten oxide-coated copper oxide nanowire arrays for enhanced activity and durability with photoelectrochemical water splitting. *J. Mater. Chem. A* **2013**, *1*, 15235−15241.

(13) Zhang, Z.; Wang, P. Highly stable copper oxide composite as an effective photocathode for water splitting via a facile electrochemical synthesis strategy. *J. Mater. Chem.* **2012**, *22*, 2456−2464.

(14) Garcia-Esparza, A.; Limkrailassiri, K.; Leroy, F.; Rasul, S.; Yu, W.; Lin, L.; Takanabe, K. Photoelectrochemical and electrocatalytic properties of thermally oxidized copper oxide for efficient solar fuel production. *J. Mater. Chem. A* **2014**, *2*, 7389−7401.

(15) Hsu, Y.; Lin, H. Photocurrent enhancement of *p*-Cu_2O thin film achieved by thermal annealing. *Int. J. Appl. Phys. Math.* **2013**, *3*, 43−45.

(16) Chauhan, D.; Satsangi, V.; Dass, S.; Shrivastav, R. Preparation and characterization of nanostructured CuO thin films for photoelectrochemical splitting of water. *Bull. Mater. Sci.* **2006**, *29*, 709−716.

(17) Bandara, J.; Udawatta, C.; Rajapakse, C. Highly stable CuO incorporated TiO_2 catalyst for photocatalytic hydrogen production from H_2O. *Photochem. Photobiol. Sci.* **2005**, *4*, 857−861.

(18) Nashim, A.; Martha, S.; Parida, K. Heterojunction conception of *n*-$La_2Ti_2O_7$/*p*-CuO in the limelight of photocatalytic formation of hydrogen under visible light. *RSC Adv.* **2014**, *4*, 14633−14643.

(19) Zhao, X.; Wang, P.; Li, B. CuO/ZnO core/shell heterostructure nanowire arrays: Synthesis, optical property, and energy application. *Chem. Commun.* **2010**, *46*, 6768−6770.

(20) Chen, L.; Shet, S.; Tang, H.; Wang, H.; Deutsch, T.; Yan, Y.; Turner, J.; Al-Jassim, M. Electrochemical deposition of copper oxide nanowires for photoelectrochemical applications. *J. Mater. Chem.* **2010**, *20*, 6962−6967.

(21) Obuchi, E.; Yamamoto, K.; Nakano, K. Transparent TiO_2 film preparation. *Kagaku Kogaku Ronbunshu* **1995**, *21*, 1075−1081.

(22) Ravirajan, P.; Peiro, A.; Nazeeruddin, M.; Gräetzel, M.; Bradley, D.; Durrant, J.; Nelson, J. Hybrid polymer/zinc oxide photovoltaic devices with vertically oriented ZnO nanorods and an amphiphilic molecular interface layer. *J. Phys. Chem. B* **2006**, *110*, 7635−7639.

(23) Wang, L.; Tacconi, N.; Chenthamarakshan, C.; Rajeshwar, K.; Tao, M. Electrodeposited copper oxide films: Effect of bath pH on

DOI: 10.1021/acssuschemeng.5b00014
ACS Sustainable Chem. Eng. 2015, 3, 710−717

grain orientation and orientation-dependent interfacial behaviour. *Thin Solid Films* **2007**, *515*, 3090−3095.
(24) Rakhshani, A.; Varghese, J. Surface texture in electrodeposited films of cuprous oxide. *J. Mater. Sci.* **1988**, *23*, 3847−3853.
(25) Wang, P.; Na, Y.; Amal, R. Embedment of anodized p-type Cu_2O thin films with CuO nanowires for improvement in photoelectrochemical stability. *Nanoscale* **2013**, *5*, 2952−2958.
(26) Elam, J. W.; Routkevitch, D.; George, S. M. Properties of ZnO/Al_2O_3 alloy films grown using atomic layer deposition techniques. *J. Electrochem. Soc.* **2003**, *150*, G339−G347.
(27) Agashe, C.; Kluth, O.; Hupkes, J.; Zastrow, U.; Rech, B.; Wuttig, M. Efforts to improve carrier mobility in radio frequency sputtered aluminium doped zinc oxide films. *J. Appl. Phys.* **2004**, *95*, 1911−1917.
(28) Gao, A.; Guan, D.; Huo, J.; Chen, J.; Yuan, C. Free standing TiO_2 nanotube array electrodes with an ultra-thin Al_2O_3 barrier layer and $TiCl_4$ surface modification for highly efficient dye sensitized solar cells. *Nanoscale* **2013**, *5*, 10438−10446.
(29) Hu, C.; Chu, K.; Zhao, Y.; Teoh, W. Efficient photoelectrochemical water splitting over anodized *p*-type NiO porous films. *ACS Appl. Mater. Interfaces* **2014**, *6*, 18558−18568.
(30) Choi, M.; Jung, J.; Park, M.; Song, J.; Lee, J.; Bang, J. Long-term durable silicon photocathode protected by a thin Al_2O_3/SiO_x layer for photoelectrochemical hydrogen evolution. *J. Mater. Chem. A* **2014**, *2*, 2928−2933.

NOTE ADDED AFTER ASAP PUBLICATION

This article was published ASAP on March 3, 2015, with minor text errors in the Results and Discussion section. The corrected version was published ASAP on March 4, 2015.

DOI: 10.1021/acssuschemeng.5b00014
ACS Sustainable Chem. Eng. 2015, 3, 710−717